

A Scalable MARL Solution for Scheduling in Conflict Graphs

Yiming Zhang and Dongning Guo

Abstract—This paper proposes a fully scalable multi-agent reinforcement learning (MARL) approach for packet scheduling in conflict graphs, aiming to minimizing average packet delays. Each agent autonomously manages the schedule of a single link over one or multiple sub-bands, considering its own state and states of conflicting links. The problem can be conceptualized as a decentralized partially observable Markov decision process (Dec-POMDP). The proposed solution leverages an on-policy reinforcement learning algorithms multi-agent proximal policy optimization (MAPPO) within a multi-agent networked system, incorporating advanced recurrent structures in the neural network. The MARL design allows for fully decentralized training and execution, seamlessly scaling to very large networks. Extensive simulations across a diverse range of conflict graphs demonstrate that the proposed solution compares favorably to well-established schedulers in terms of both throughput and delay under various traffic conditions.

Index Terms—Decentralized partially observable Markov decision process; dynamic traffic; multi-agent reinforcement learning (MARL); recurrent neural networks; wireless networks.

I. INTRODUCTION

This paper addresses the challenge of scheduling in conflict graphs, a crucial problem with broad applications across various domains [1], [2]. This problem involves allocating resources like spectrum and time slots to conflicting tasks or events while considering both dependencies and constraints. In wireless communication networks, using conflict graphs to represent interference between different links offers a straightforward abstraction, directly addressing the fundamental challenges inherent in these networks. Our goal is to develop a distributed, efficient and scalable method for scheduling the transmissions of wireless links that interfere with each other across multiple frequency sub-bands.

Srikant et al. [3] demonstrated the throughput optimality of the general MaxWeight algorithm for certain conflict graphs settings. However, one limitation of the MaxWeight algorithm lies in its requirement of finding a full set of maximum independent sets. This task is proven to be NP-complete [4]. Here, a maximum independent set refers to a group of links that can transmit packets simultaneously without collisions, and no additional links can be added without causing interference. Simpler methods like Longest-Queue-First (LQF) reduce complexity but they often support only a portion of the capacity region in general graphs. Both MaxWeight and

LQF are centralized, which is impractical in modern communication networks due to the growing number of devices and the need for low latency, as centralized processing can be time-consuming. Consequently, developing a distributed and scalable scheduling method becomes imperative. To address this issue, Srikant et al. proposed a low-complexity distributed method called queue-length-based CSMA (Q-CSMA) [5], offering a practical solution in distributed environments. We use it as one of the benchmarks in our simulation. In a more recent study, Zhao et al. [2] adopted graph neural networks, leveraging topological information to address similar scheduling problems in conflict graphs, showcasing the potential of machine learning in enhancing scheduling strategies.

The aforementioned works and previous research like [6] have primarily focused on maximizing the throughput due to its tractability. This trend continues in recent machine learning-based scheduling studies, such as those in [2], [7], [8], where sum-rate is the primary evaluation metric. In this work, we adopt the average packet delay as the quality of service (QoS) metric for two main reasons. First, practical wireless networks often operate at substantially lighter traffic loads than the maximum achievable throughput, making latency a more accurate indicator of user experience. Second, while achieving high throughput is essential for low-latency experiences, it is possible to have significant packet delays even with high throughput, for instance in cases of unbalanced scheduling where certain links are favored consistently.

Formulating a tractable minimization problem based on average packet delays without compromising throughput optimality has posed a longstanding challenge. This paper adopts a data-driven model-free approach, leveraging reinforcement learning (RL). Compared with traditional method aiming at optimizing some objective function, RL method offers three key advantages. First, it sidesteps the difficulty of directly formulating the problem around average packet delay minimization, and the associated computational costs in potential high-dimensional, non-convex optimization. Second, RL-based scheduling benefits from historical states and interactions, providing a more comprehensive understanding of system dynamics over time than methods which focus on optimizing objectives based on the current system state alone. Third, this historical perspective also enables consideration of long-term utility in decision-making processes.

In recent years, RL has gained significant traction as a successful tool in diverse domains such as game play, robotics, autonomous driving, and wireless networks [9]. Multi-agent reinforcement learning (MARL) expands the scopes of RL by

The authors are with Department of Electrical and Computer Engineering, Northwestern University, Evanston, IL 60208, USA.

The work was supported in part by the National Science Foundation under grant No. 2003098, a gift from Intel Corporation, and also the SpectrumX Center (NSF grant No. 2132700).

introducing multiple agents that interact and learn collectively to achieve desirable rewards. In this work, we employ the MARL framework to tackle the scheduling problem in conflict graphs. Each individual link is represented as an agent within the MARL framework. These agents collaborate, learning and making decisions collectively to optimize scheduling while considering the interference constraints inherent in networked systems.

Developing a scalable MARL solution for practical wireless networks is challenging due to the exponentially large joint-action space. Methods like independent learners [10] can be effective but may face instability [11]. To address the expansive Q -table in temporal difference learning, function approximation techniques like linear methods [12] and neural networks [13] have been explored. Our earlier work [14] utilized centralized training with distributed execution, yielding promising results in up to 20-agent scenarios. Beyond scalability, another challenge arises from the limited information exchange in a practical network. This limitation, often due to communication constraints or intolerable delays, means that agents only have access to local observations about their immediate environment. Consequently, agents must learn local policies that map their local observations to local actions, necessitating a distributed approach.

To address scalability and the need for decentralization, we approach MARL in conflict graphs as distributed learning in a Decentralized Partially Observable Markov Decision Process (Dec-POMDP) framework. We employ a widely adopted on-policy algorithm multi-agent proximal policy optimization (MAPPO) and integrate recurrent structures in the neural network. These recurrent structures enable agents to better estimate the underlying state by encoding historical transitions. Additionally, we modify the centralized training and distributed execution paradigm, using only local information for both training and execution. This key change significantly enhances scalability, keeping training costs constant regardless of agent numbers. This scalability is vital in practice where network size can vary, ensuring that our solution is adaptable to a wide range of scenarios without compromising on efficiency or effectiveness.

MARL's application in networked systems, with agents relying on local observations, has been a major research focus [7], [15], [16]. Unlike in [15], [16], which assumes a decomposable transition probability distribution such that one agent's state transition is independent of other agents' actions, here we assume full dependence on neighboring agents' actions. This dependence is necessary to model the need of retransmissions due to collisions.

This paper presents several key contributions:

- We formulate the scheduling problem in conflict graphs, driven by traffic considerations, as a distributed learning problem aimed at minimizing average packet delay;
- We employ MAPPO and recurrent neural network structures for distributed scheduling, and compare individual agent training with shared policy implementation to assess computational efficiency

- We enhance the conventional centralized training and distributed execution to keep the training cost and the policy network size constant for each agent regardless of the number of agents in the system, thus significantly improving scalability.
- We conduct extensive simulations on distinct conflict graphs to validate the performance and scalability of our approach. Additionally, we investigate the robustness in the face of traffic mismatch between training and testing conditions.

The remainder of this paper is organized as follows. We formulate the learning problem in Section II. In Section III, we introduce an RL framework. In Section IV, we discuss the simulation setup and numerical results. Concluding remarks are given in Section V.

II. SYSTEM MODEL AND PROBLEM FORMULATION

A. State, Action, and Reward

In this study, we focus on decentralized partially observable DEC-POMDPs in a networked system. Consider a network of N agents, whose indexes form a set $\mathcal{I} = \{1, \dots, N\}$. Let $\mathcal{N}(n) \subset \mathcal{I}$ denote agent n 's neighborhood, which includes the agent itself. (As an example, as an agent, a link's neighborhood could consist of all links that it has conflicts with. The neighborhood of an agent can also be defined more generally as an arbitrary subset of agents.) Let \mathcal{S}_n denote the local state space of agent n . Let the global state space be denoted as $\mathcal{S} = \mathcal{S}_1 \times \dots \times \mathcal{S}_N$. Let $s = (s_1, \dots, s_N) \in \mathcal{S}$ denote the global state at a given point in time; then the observation of agent n be denoted as $O_n(s) = (s_i, i \in \mathcal{N}(n))$. This local observation provides a partial representation of the global state s . Let $\mathcal{A} = \mathcal{A}_1 \times \dots \times \mathcal{A}_N$ represent the joint action space of all agents. In each transition, agent n selects an action $a_n \in \mathcal{A}_n$ based on its observation. Let $P(s' | s, A)$ represent the transition probability from state $s \in \mathcal{S}$ to $s' \in \mathcal{S}$ given the joint action $A = (a_1, \dots, a_N) \in \mathcal{A}$. The reward function of agent n is denoted as $R_n(s, A)$.

B. Conflict Graph

Consider an undirected conflict graph denoted as $\mathcal{G} = (\mathcal{I}, \mathcal{E})$, where each vertex in \mathcal{I} represents a wireless link, and an edge $(i, j) \in \mathcal{E}$ with $i, j \in \mathcal{I}$ and $i \neq j$ indicates link i and link j cause interference to each other. Time is considered in discrete slots. Each link is equipped with a first-in-first-out (FIFO) queue. Let $K_n^{(t)}$ denote the number of newly arrived packets to link n at the beginning of time slot t . It is assumed that $K_n^{(t)}$ is independent across all links n and time slot t and all packets are identical. Furthermore, we model the traffic on each link as a discrete-time memoryless Poisson process, as described by the following equation:

$$\Pr(K_n^{(t)} = k) = \frac{\lambda_n^k}{k!} e^{-\lambda_n} \quad (1)$$

A successful packet transmission on a specific sub-band by a link during a time slot occurs only if no other conflicting link transmits on the same sub-band in that slot. Without loss

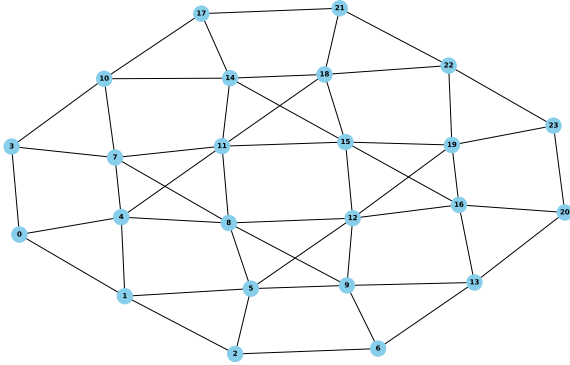


Fig. 1. Conflict graph of 24 links abstracted from 24-link grid network in [5].

of generality, we assume that all links have unit capacity on each sub-band, i.e., a scheduled link can transmit one packet using one sub-band in one time slot if transmission successful. Let S represent the total number of sub-bands, and let $m_{n,h}^{(t)}$ be the schedule of link n on h -th sub-band in time slot t . Specifically, $m_{n,h}^{(t)} = 1$ indicates that link n is scheduled for conflict-free transmission on the h -th sub-band at time slot t . If there is a conflict or the link is not scheduled for transmission, then $m_{n,h}^{(t)} = 0$. Given these assumption, we can accurately represent queueing dynamic for each link. The queue length of link n at the end of slot t is expressed as follows:

$$q_n^{(t)} = \max \left(0, q_n^{(t-1)} + K_n^{(t)} - \sum_{h=1}^S m_{n,h}^{(t)} \right). \quad (2)$$

We assume that $q_n^{(0)}$ is set to 0 since the queue starts empty at the beginning. This traffic model represents a significant simplification of wireless networks, aimed at validating the effectiveness of the multi-agent RL algorithm with partial observation.

Fig. 1 depicts a conflict graph, where each of the 24 vertices represents a link, and each edge represents a conflict between two links. The interference is always mutual between pairs of links and neighborhood of agents can be defined as 1-hop neighbors, this graph is equivalent to the 24-link grid network introduced in [5, Fig. 1],

C. QoS and Problem Formulation

For agent n , we express the total discounted reward of a given trajectory of the state and action from time t onward as:

$$\sum_{\tau=0}^{\infty} \gamma^{\tau} R_n^{(t+\tau+1)} \left(s^{(t+\tau)}, a^{(t+\tau)} \right). \quad (3)$$

The control policy of an agent, denoted as π_{n,θ_n} , maps the observation $O_n(s) = (s_i, i \in \mathcal{N}(n))$ to the action a_n . For every agent $n \in \{1, \dots, N\}$ and sub-band $h \in \{1, \dots, S\}$, the control policy decision variable $m_{n,h}^{(t)}$ is a binary variable that indicates the agent n 's decision on sub-band h in time slot

t . The policy π_{n,θ_n} , which is a neural network parameterized by weights θ_n , is trained using a collection of state, action, and reward trajectories. In this work, all agents are trained in parallel synchronously. The idea is that once trained, the agents will have learned proficient policies that lead to highly desirable total reward.

In this work, we adopt the average packet delay as the key performance aligning closely QoS measure used in practice. This metric provides valuable insights beyond what throughput measurements alone can offer. We observe that insufficient throughput results in heightened average packet delays. Evidently, the longer the links' queue lengths are, the larger the packet delays are. This motivates us to define learning objectives using the queueing states. Specifically, the direct contribution of agent n to the queue length objective can be expressed as:

$$u_n^{(t)} = -q_n^{(t)}. \quad (4)$$

To prevent agents from adopting overly aggressive transmission strategies that could cause interference to other agents, we include the queue lengths of agent n 's neighbors as indirect contributions. This encourages agents to collaborate with others and make joint decisions that lead to mutually beneficial outcomes. The agent n 's reward function is the cumulative queue length of itself and its neighbors in time slot t defined as:

$$R_n^{(t)}(s_{\mathcal{N}(n)}, a_{\mathcal{N}(n)}) = u_n^{(t)} + \sum_{i \in \mathcal{N}(n), i \neq n} u_i^{(t)}. \quad (5)$$

Our primary objective is to develop an algorithm that generates a sequence of joint device scheduling decisions across the network, aiming at reducing the queue length of agents. By considering the cumulative queue lengths of agent n and its neighbors, the reward function promotes collaborative decision-making among the agents. Agents are encouraged by reward function to make jointly good decisions that optimize not only their own queue lengths but also positively influence the queue lengths of neighboring agents, thereby reducing overall network congestion and leading to improved system performance.

III. A REINFORCEMENT LEARNING FRAMEWORK

In this paper, we adopt a multi-agent reinforcement learning setting where agents interact with an unknown environment in discrete time steps to acquire a policy. We employ an effective on-policy algorithm MAPPO, which has demonstrated success in solving various cooperative multi-agent tasks [17].

We consider two different training methods. In the first method, we use MAPPO to train a separate pair of actor and critic networks for each agent. Since agents see different neighborhoods in the conflict graph and may in general have distinct traffic situations, this approach ensures a highly customized and effective policy for each agent.

As an alternative, the second method trains a shared neural network as a unified policy for all agents. The reward in this case would be the average reward of all agents. While this

shared policy approach may result in performance degradation compared to the individualized training, it reduces the computational complexity substantially. Preliminary results indicate that, despite this performance trade-off, the shared policy remains remarkably effective, surpassing several established benchmarks. This shared approach is particularly efficient in scenarios where agents are homogeneous, sharing similar local topology and traffic conditions.

A. Actor Network

The actor network, parameterized by θ , represents the policy π_θ for each agent. It maps the local observation s_n to a categorical distribution over discrete actions in our specific setting. Let θ_{old} denote the parameter values of the policy network from the previous iteration. Let B represent the training batch size. For agent n and time i in a batch, we define

$$r_{\theta,n}^{(i)} = \frac{\pi_\theta \left(a_n^{(i)} \mid s_n^{(i)} \right)}{\pi_{\theta_{\text{old}}} \left(a_n^{(i)} \mid s_n^{(i)} \right)}. \quad (6)$$

Let $H(\cdot)$ denote the Shannon entropy of a probability mass function. The objective of the actor is to maximize the following function:

$$J(\theta) = \frac{1}{BN} \sum_{i=1}^B \sum_{n=1}^N \min \left(r_{\theta,n}^{(i)} A_n^{(i)}, c_\epsilon \left(r_{\theta,n}^{(i)}, 1 \right) A_n^{(i)} \right) + \sigma \frac{1}{BN} \sum_{i=1}^B \sum_{n=1}^N H \left(\pi_\theta \left(\cdot \mid s_n^{(i)} \right) \right) \quad (7)$$

where

$$c_\epsilon(x, y) = \min(\max(x, y - \epsilon), y + \epsilon) \quad (8)$$

represents a clipping function, the advantage function $A_n^{(i)}$ is computed using the generalized advantage estimation (GAE) method, and σ denotes a hyperparameter.

B. Critic Network

The critic network in MAPPO, parameterized by ϕ , is responsible for evaluating the value function $V_\phi(s)$, which estimates the expected return from a given state. The training objective of the critic network is to minimize the loss function:

$$L(\phi) = \frac{1}{BN} \sum_{i=1}^B \sum_{n=1}^N \max \left[\left(V_\phi \left(s_n^{(i)} \right) - \hat{R}^{(i)} \right)^2, \left(c_\epsilon \left(V_\phi \left(s_n^{(i)} \right), V_{\phi_{\text{old}}} \left(s_n^{(i)} \right) \right) - \hat{R}^{(i)} \right)^2 \right] \quad (9)$$

where $\hat{R}^{(i)}$ represents the discounted reward-to-go, which is defined as the cumulative sum of discounted rewards from a specific time slot t until the end of an episode.

C. Recurrent Structure

In POMDPs, the recurrent structure plays a vital role due to the limited information provided by a single local observation, which may not be sufficient for the agent to fully comprehend the dynamics of the environment. Through experimentation, it was observed that algorithms like multi-agent deep deterministic policy gradient (MADDPG) [13] struggle when using local observations only, whereas they perform well when provided with global information.

By incorporating a recurrent structure, such as LSTM or GRU, the agent can effectively integrate current observations with past observations and actions. This integration enables the agent to update its internal state representation and maintain an accurate estimation of the underlying state. The inclusion of sequential memory allows the agent to learn and recognize patterns while capturing the dynamic nature of the environment. Additionally, the memory-based architecture empowers the agent to make informed decisions by considering the long-term consequences of its actions and leveraging the accumulated knowledge stored within the memory.

In our implementation, both the actor and critic networks are recurrent neural networks (RNNs). Specifically, we take a sum of the loss function defined in (9) over time. In addition, the input to both the actor and critic networks includes the RNN states. We train these networks using back-propagation through time (BPTT), a technique specifically designed for training RNNs. A detailed pseudocode illustrating the training phase is found in [17]. During the training phase, all actor and critic networks are updated for a fixed number of steps for each training episode.

D. Decentralized Training and Distributed Execution

The paradigm of centralized training and distributed execution is widely adopted to address challenges of non-stationarity and scalability. Under this paradigm, global information is used in the training stage to enhance the learning phase, whereas agents rely solely on local information during execution. The conventional MAPPO follows this paradigm, where the computation of the value function $V_\phi(s)$ during training uses the global state s as input to the critic network. However, it is impractical for a central controller to gather timely global information in many real-world scenarios.

To overcome the scalability limitations, we draw from the scalable framework suggested in [15] to propose a modification to the centralized training paradigm. We provide the critic network with local information as input in lieu of the global state. Specifically, for each agent n , the critic network n is fed with its local observation O_n , which contains the information of itself and its neighboring agents. This adjustment ensures full scalability as the training cost per agent remains constant and does not escalate with an increase in the number of agents.

E. State Space and Action Space Design

Following the Dec-POMDP framework, the global state in time slot t can be represented as $s^{(t)} = \left(s_1^{(t)}, \dots, s_N^{(t)} \right)$,

where $s_n^{(t)} = q_n^{(t-1)} + K_n^{(t)}$. This representation signifies the queue length of agent n at the moment of measuring the local observation. Specifically, $q_n(t-1)$ represents the queue length of link n at the end of time slot $t-1$, while $K_n^{(t)}$ defined in (1) represents the arrival of new packets at the beginning of time slot t . In our Dec-POMDP setting, an agent only has access to information about itself and its neighboring agents. Therefore, the local observation $O_n^{(t)}(s)$ can be defined as $O_n^{(t)}(s) = (s_i^{(t)}, i \in \mathcal{N}(n))$. Clipping is employed here to make the observation to be a coarsely quantized function of the queue length, which guarantee the state space to be finite.

The action space dimension for each agent is determined by the number of sub-bands, S . The action decision that agent n needs to make consists of S binary variables. Consequently, there are 2^S possible actions available to each agent. If S is not too small, the large action space renders tabular reinforcement learning methods impractical [16].

In our problem, the agent must determine the allocation of sub-bands from 1 to S in each time slot to transmit its packets. The objective is to transmit as many packets from the queue as possible while minimizing conflicts with neighboring links. The agent's decision-making process revolves around selecting the appropriate sub-bands and their respective usage to optimize its transmission performance, taking into account the constraints imposed by neighboring agents' actions.

IV. SIMULATION RESULTS AND ANALYSIS

A. Simulation Setup

The performance of the proposed MARL-based scheduler is evaluated and compared in terms of QoS against two benchmarks. The first benchmark scheme, referred to as local longest queue (LLQ), schedules a link for transmission if it has a longer queue than all links that it has a conflict with; in case of a tie between multiple links, each link is scheduled with probability $1/2$ independently. The second benchmark scheme is Q-CSMA [5], where links perform carrier sensing prior to transmission, ensuring that all scheduled links form an independent set, and then each enabled link transmits with a certain probability, where the probability is updated based on its queue length. Regardless of the scheduler, a collision occurs when multiple links transmit packets simultaneously on the same sub-band in the same time slot, where the failed packets remain in their respective queues.

We consider one scenario with a single channel and a second scenario with multiple (three) sub-bands. We also test algorithms where agents share the same centrally trained policy as well as algorithms where agents train separate policies.

The experiments are conducted on three distinct sets of graphs:

- 1) The conflict graph depicted in Fig. 1, where each of the 24 vertices represents a link. The graph is equivalent to the 24-link grid network introduced in [5, Fig. 1], and we test under the same traffic conditions.
- 2) Randomly generated conflict graphs where each link has conflicts with two to four other links. Specifically, we

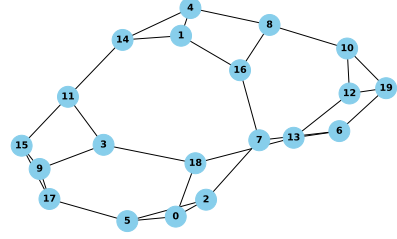


Fig. 2. conflict graph of 20 links

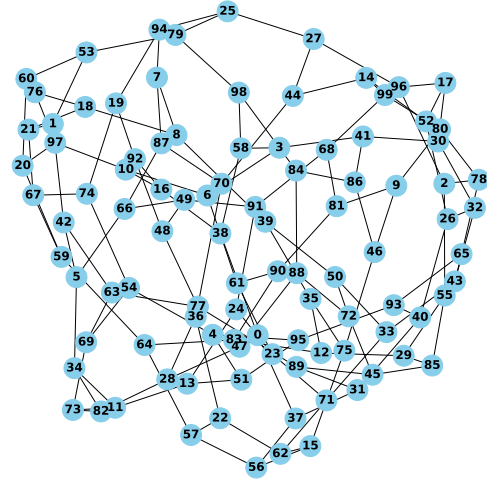


Fig. 3. conflict graph of 100 links

use a 20-link graph depicted in Fig. 2 and a 100-link graph depicted in Fig. 3.

- 3) A conflict graph as an abstraction of a cellular network depicted in Fig. 4. Here each user device (UE) has a direct link to its nearest access point (AP). Two direct links are in conflict if their mutual interference, determined by path losses, exceeds a certain threshold.

B. Training and Testing

During the training phase, we set the duration of an episode to 1,000 time slots. Whenever the queue length of any link surpasses a predefined threshold, it signifies a congested or very unfavorable traffic situation. In such instances, the current episode is curtailed, and a new episode is started. The purpose here is to avoid being trapped in adverse queuing conditions before the scheduler is trained well. Furthermore, the implementation of this threshold ensures that the state space remains finite, thereby enabling the problem to be effectively solved using reinforcement learning techniques.

During testing or deployment, we adopt average packet delay as the metric to evaluate the QoS performance. We

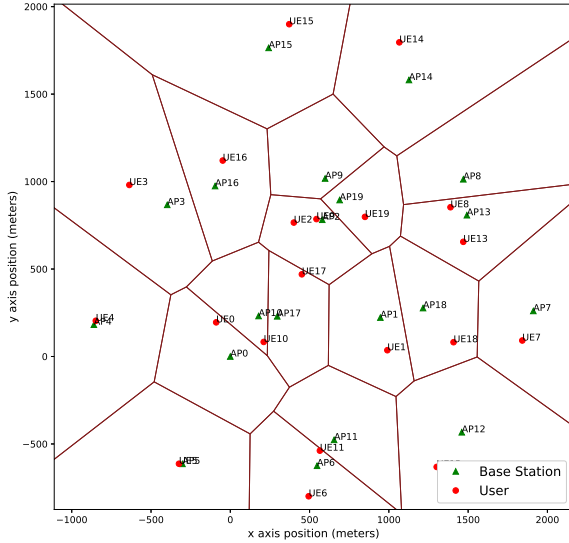


Fig. 4. A cellular network with 20 access points (APs) and 20 user devices (UEs).

set the duration of a testing episode to 5,000 time slots. To determine the average packet delay for a single episode, we calculate the average delay of successfully transmitted packets within these 5,000 time slots if the queue is perceived to be stable.

C. Single Frequency Band

In this subsection, we assume all agents share a single frequency band. We present the average packet delay obtained from many episodes.

We first simulate the 24-link grid network in Fig. 1, where the link arrival rates are a linear combination of arrivals to four maximum independent sets [5, Sec. VI.A with $\rho = 0.2$]. Fig. 5 demonstrates that, across all 24 links, the average packet delay using the MARL method is substantially lower than the benchmarks. When also averaged over links, the packet delay of the MARL method with a shared policy is 1.49, which is 30% less than that of Q-CSMA (2.14) and 38% than that of LLQ (2.42). If agents use separately trained policies, the average delay is even smaller at 1.19.

With the 20-link graph in Fig. 2, we test our algorithms under a light, a medium, and a heavy traffic condition, which poses increasing challenges to the learning method (Fig. 6). In the light traffic scenario, the MARL method, utilizing separate and shared policy approaches, exhibited average packet delays of 1.17 and 1.31 time slots, respectively. This performance translates to an improvement of approximately 51.0% over the Q-CSMA method (2.39) and 37.8% over the LLQ approach (1.88). As traffic intensity escalates, the corresponding delays increase. Under medium traffic conditions, the MARL framework's separate and shared policies result in average delays of

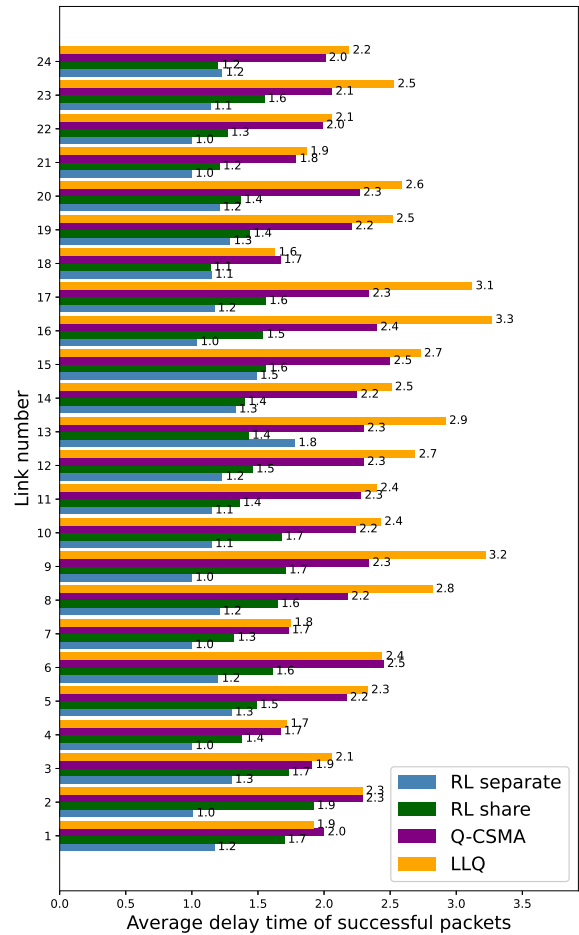


Fig. 5. QoS performance of 24-link grid network in [5] with single channel under light traffic.

1.24 and 2.3 time slots, respectively. These figures represent a notable enhancement of 66.7% compared to Q-CSMA (3.72) and 77.0% over LLQ (5.38).

As traffic intensity escalates, Fig. 6 demonstrates that all four algorithms exhibit increased average delays, albeit at differing rates. In the case of a heavy traffic condition experimented here, which is relatively close to the boundary of the capacity region, the LLQ benchmark algorithm experiences significant challenges, resulting in an average packet delay of up to 67.72 time slots. The Q-CSMA scheduler is still stable and results in average packet delay of 4.9 time slot. Remarkably, our MARL method with separate policies achieves a 1.37 time slot average delay, a substantial 70% reduction compared to Q-CSMA. However, the shared policy variant of the MARL method exhibits instability under such intense traffic.

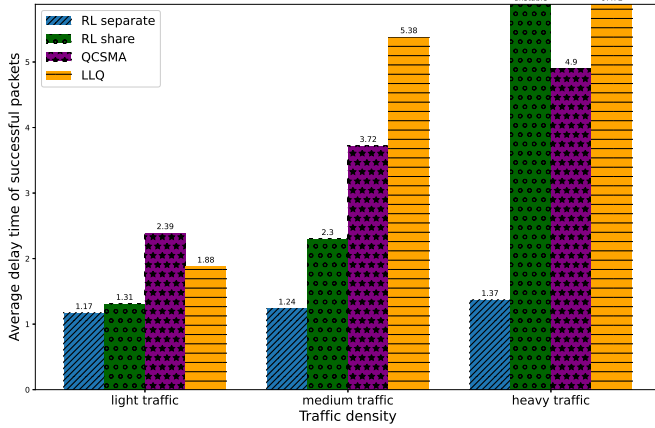


Fig. 6. QoS performance of 20-link conflict graph with single channel under varying traffic loads.

TABLE I
AVERAGE PACKET DELAYS IN THE 20-LINK CELLULAR NETWORK IN DIFFERENT TRAFFIC LOADS.

Traffic load	separate policy	LLQ	Q-CSMA
light	1.08	1.37	1.45
medium	1.18	2.24	1.80

We also simulate the MARL-based solution in a conflict graph as an abstraction of the cellular network depicted in Fig. 4. The path loss of a link is determined by its length d in kilometers according to $128.1 + 37.6 \log_{10} d$ in dB. A typical link has conflicts with up to three other links, e.g., AP0 serving UE0 is in conflict with AP17 serving UE17. Several links do not have conflicts, e.g., AP15 serving UE15. We omit the conflict graph here. Since links can have very different interference environments, we let agents train their separate policies. As shown in Table I, the trained policies outperform the benchmarks under light and medium traffic conditions.

TABLE II
AVERAGE PACKET DELAYS IN THE 20-LINK CONFLICT GRAPH IN DIFFERENT SCENARIOS.

	separate policies	shared policy	LLQ benchmark
single channel	1.17	1.31	1.88
three sub-bands	1.01	1.28	2.15

TABLE III
AVERAGE PACKET DELAYS IN THE 100-LINK CONFLICT GRAPH IN DIFFERENT SCENARIOS.

	shared policy	LLQ benchmark
single channel	1.27	2.00
three sub-bands	1.04	2.24

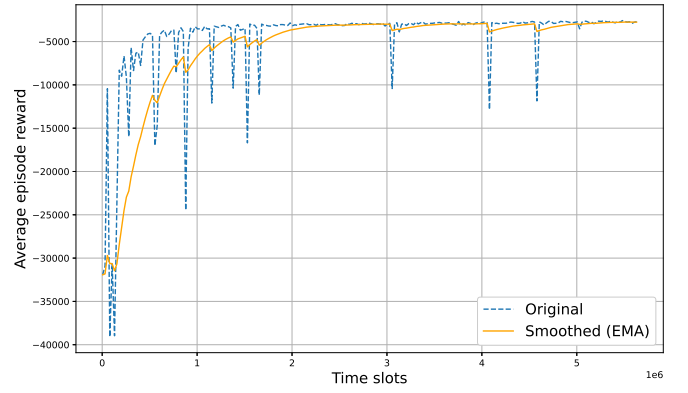


Fig. 7. Reward of training episodes with a shared policy.

D. Multiple Sub-bands

We compare the average packet delays attained by the MARL method and the LLQ benchmark. Since Q-CSMA was proposed for a single channel, it is not included here as a benchmark. QoS results for the 20-link graph in Fig. 2 are presented in Table II. The average delays of both the separate and shared policies are lower than that of the LLQ benchmark. For the 100-link graph in Fig. 3, the QoS results in Table III demonstrate the superiority of the MARL method with a shared policy.

The preceding results demonstrate that, with either a single band or multiple sub-bands, our approach consistently outperforms the benchmark algorithm, often achieving less than half the average delay compared to the benchmark. A close examination of the agents' policies reveals that their joint policy almost always schedules an independent set that includes the longest queues on every sub-band.

E. Scalability

Table III also validates the proposed MARL method in a moderately large graph with 100 links. Here we only simulated the method where a single policy is trained and shared by all 100 agents. While we have not simulated the 100-link conflict graph with 100 separately trained agents due to its running time, the computational complexity per agent remains constant. It is conceivable that such a solution with a distributed implementation scales very well with the graph size.

F. Policy Convergence

With the 20-link conflict graph, we test the learned policies once every five training episodes and plot the rewards. The average reward from the MARL method using a shared policy is depicted as the blue dashed line in Fig. 7. This figure also incorporates a smooth curve generated using the exponential moving average (EMA) method for better clarity. It is evident that the average reward exhibited a consistent improvement during the initial stages of training and eventually stabilized after about two million time slots. This indicates that each

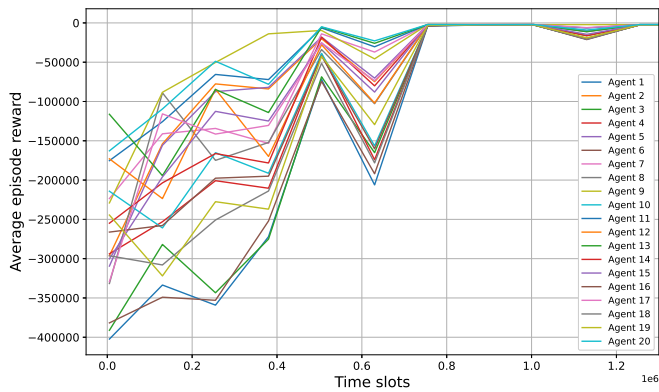


Fig. 8. Rewards of training episodes with separate policies.

TABLE IV
TRAINING AND TESTING MISMATCH.

Traffic load for testing:	Light	Medium	Heavy
if trained under light traffic:	good	mixed	unstable
if trained under medium traffic:	good	good	unstable
if trained under heavy traffic:	good	good	good

agent has successfully acquired a proficient policy. The occasional spikes in rewards during later stages, attributable to exploration in MARL methods, were quickly followed by a return to stable rewards.

Applying the MARL method using separate policies to the same 20-link graph, the 20 agents' rewards are plotted in Fig. 8. In this case, we note that the method with separate policies exhibits larger variability in early stages, but all agents' reward trends upward in general, and they converge to efficient policies somewhat more rapidly than the shared policy approach.

G. Training and Testing Mismatch

We also investigate the robustness of the MARL method when trained and tested under mismatched traffic conditions. We characterize the performance as "unstable" if the queue lengths are observed to generally increase persistently. Conversely, the performance is deemed "good" if it demonstrates satisfactory QoS performance when compared to the benchmark. The term "mixed" is used to describe a mixture of both "good" and "unstable" performance amongst the agents.

Table IV demonstrates that policies trained under heavier traffic loads exhibit better performance when handling lighter traffic loads. For instance, policies trained in heavy traffic loads demonstrate satisfactory behavior in both light and medium traffic environments. Conversely, policies trained in light traffic loads show inadequate performance under medium and heavy traffic conditions.

V. CONCLUSION

We have introduced a novel multi-agent deep reinforcement learning framework for addressing the distributed scheduling problem in partially observable conflict graphs. This framework effectively addresses a common challenge of solving

Dec-POMDP problems. Our proposed method adopts a "modified" centralized training and distributed execution paradigm and the design is highly scalable.

The simulation results showcase the effectiveness of the trained policy in achieving significantly improved QoS and throughput region compared to well-known schedulers. Furthermore, the proposed method exhibits remarkable robustness in adapting to variations in conflict graph sizes and densities, further validating its efficacy in practical deployment scenarios. The proposed framework is potentially applicable to a broader set of resource allocation problems.

REFERENCES

- [1] A. A. Al-Habob, O. A. Dobre, A. G. Armada, and S. Muhaidat, "Task scheduling for mobile edge computing using genetic algorithm and conflict graphs," *IEEE Transactions on Vehicular Technology*, vol. 69, no. 8, pp. 8805–8819, 2020.
- [2] Z. Zhao, G. Verma, C. Rao, A. Swami, and S. Segarra, "Distributed scheduling using graph neural networks," in *ICASSP 2021-2021 IEEE International Conference on Acoustics, Speech and Signal Processing (ICASSP)*. IEEE, 2021, pp. 4720–4724.
- [3] R. Srikant and L. Ying, *Communication networks: an optimization, control, and stochastic networks perspective*. Cambridge University Press, 2013.
- [4] R. E. Tarjan and A. E. Trojanowski, "Finding a maximum independent set," *SIAM Journal on Computing*, vol. 6, no. 3, pp. 537–546, 1977.
- [5] J. Ni, B. Tan, and R. Srikant, "Q-CSMA: Queue-length-based CSMA/CA algorithms for achieving maximum throughput and low delay in wireless networks," *IEEE/ACM Transactions on Networking*, vol. 20, no. 3, pp. 825–836, 2011.
- [6] K. Shen and W. Yu, "Fractional programming for communication systems—part i: Power control and beamforming," *IEEE Transactions on Signal Processing*, vol. 66, no. 10, pp. 2616–2630, 2018.
- [7] K. Yang, D. Li, C. Shen, J. Yang, S.-p. Yeh, and J. Sydir, "Multi-agent reinforcement learning for wireless user scheduling: Performance, scalability, and generalization," in *2022 56th Asilomar Conference on Signals, Systems, and Computers*. IEEE, 2022, pp. 1169–1174.
- [8] O. Orhan, V. N. Swamy, M. Rahman, H. Nikopour, and S. Talwar, "Graph neural networks to enable scalable mac for massive mimo wireless infrastructure," in *2023 International Conference on Artificial Intelligence in Information and Communication (ICAIIIC)*. IEEE, 2023, pp. 489–494.
- [9] Y. S. Nasir and D. Guo, "Multi-agent deep reinforcement learning for dynamic power allocation in wireless networks," *IEEE Journal on Selected Areas in Communications*, vol. 37, no. 10, pp. 2239–2250, 2019.
- [10] C. Claus and C. Boutilier, "The dynamics of reinforcement learning in cooperative multiagent systems," *AAAI/IAAI*, vol. 1998, no. 746-752, p. 2, 1998.
- [11] L. Matignon, G. J. Laurent, and N. Le Fort-Piat, "Independent reinforcement learners in cooperative markov games: a survey regarding coordination problems," *The Knowledge Engineering Review*, vol. 27, no. 1, pp. 1–31, 2012.
- [12] K. Zhang, Z. Yang, H. Liu, T. Zhang, and T. Basar, "Fully decentralized multi-agent reinforcement learning with networked agents," in *International Conference on Machine Learning*. PMLR, 2018, pp. 5872–5881.
- [13] R. Lowe, Y. I. Wu, A. Tamar, J. Harb, O. Pieter Abbeel, and I. Mordatch, "Multi-agent actor-critic for mixed cooperative-competitive environments," *Advances in neural information processing systems*, vol. 30, 2017.
- [14] Y. Zhang and D. Guo, "Distributed MARL for scheduling in conflict graphs," in *2023 59th Annual Allerton Conference on Communication, Control and Computing*. IEEE, 2023.
- [15] G. Qu, A. Wierman, and N. Li, "Scalable reinforcement learning of localized policies for multi-agent networked systems," in *Learning for Dynamics and Control*. PMLR, 2020, pp. 256–266.
- [16] H. Wei, X. Liu, W. Wang, and L. Ying, "Sample efficient reinforcement learning in mixed systems through augmented samples and its applications to queueing networks," *arXiv preprint arXiv:2305.16483*, 2023.

- [17] C. Yu, A. Velu, E. Vinitzky, J. Gao, Y. Wang, A. Bayen, and Y. Wu, “The surprising effectiveness of ppo in cooperative multi-agent games,” *Advances in Neural Information Processing Systems*, vol. 35, pp. 24 611–24 624, 2022.